J Mater Sci: Mater Electron (2018) 29:1298–1303
DOI 10.1007/s10854-017-8035-7

Microwave dielectric properties of low-fired $[Mg_{0.98}(Li_{0.5}Bi_{0.5})_{0.02}]_2SiO_4$–$Ca_{0.8}Sm_{0.4/3}TiO_3$ composite ceramics

Simei Zhai[1] · Peng Liu[1] · Zhifen Fu[1]

Received: 16 August 2017 / Accepted: 11 October 2017 / Published online: 26 October 2017

Abstract $[Mg_{1-x}(Li_{0.5}Bi_{0.5})_x]_2SiO_4$ (MLBS, $0 \le x \le 0.06$) ceramics were fabricated via a conventional solid-state reaction method. The X-ray diffraction showed that a single forsterite phase was formed while the sintering temperature of MLBS ceramics was lowed. The $(1-y)[Mg_{0.98}(Li_{0.5}Bi_{0.5})_{0.02}]_2SiO_4$–$yCa_{0.8}Sm_{0.4/3}TiO_3$ (MLBS2-CST, $0.05 \le y \le 0.2$) composite ceramics added with 4 wt% LiF were well sintered from 850 to 950 °C. With increasing $Ca_{0.8}Sm_{0.4/3}TiO_3$ composition (y), τ_f values increased from negative to positive. The 0.85MLBS2-0.15CST-4 wt% LiF composite ceramics sintered at 875 °C exhibited excellent microwave dielectric properties of $\varepsilon_r = 11.9$, $Q \times f = 12{,}000$ GHz, and $\tau_f = 4.9$ ppm/°C. Such sample was compatible with Ag electrodes, which indicates the ceramic is a promising material for LTCC application.

1 Introduction

Nowadays, low-temperature co-fired ceramic (LTCC) has been giving rise to considerable interest to cater the requirement of miniaturization and integration [1, 2]. The microwave dielectric materials used in LTCC field are required to have low sintering temperature (< 960 °C), suitable permittivity (ε_r), high quality factor ($Q \times f$) value, a near-zero temperature coefficient of resonant frequency (τ_f) and co-fired well with Ag electrodes [3, 4]. Therefore, looking for a potential LTCC material is an instant task in the last few years.

✉ Peng Liu
liupeng@snnu.edu.cn

[1] College of Physics and Information Technology, Shaanxi Normal University, Xi'an 710062, China

Forsterite (Mg_2SiO_4) ceramics exhibited excellent microwave dielectric properties of $\varepsilon_r \sim 7.0$, $Q \times f \sim 230{,}000$ GHz and $\tau_f \sim -65$ ppm/°C [5]. However, high sintering temperature (around 1500 °C) and large negative temperature coefficient of resonant frequency ($\tau_f \sim -65$ ppm/°C) restricted their further application. Some investigations have been done to reduce the sintering temperature and improve the τ_f value. Up to date, several researchers have reported on the microwave dielectric properties of the partial substitution of the A-site or B-site in Mg_2SiO_4 ceramic system [6, 7]. Zhang et al. reported the $(Mg_{1-x}Ni_x)_2SiO_4$ ceramics for $x = 0.05$ doped with 12 wt% Li_2CO_3–V_2O_5 sintered at 1150 °C exhibited good microwave dielectric properties: $\varepsilon_r = 6.9$, $Q \times f = 99{,}800$ GHz, and $\tau_f = -50$ ppm/°C [6]. In addition, some positive τ_f values materials, such as TiO_2, $Ca_{0.9}Sr_{0.1}TiO_3$, $Ba_3(VO_4)_2$ and $(La_{0.5}Na_{0.5})TiO_3$, have been used to tune τ_f value of Mg_2SiO_4 ceramics [8–11]. Gang Dou et al. reported that 0.91 Mg_2SiO_4–0.09 $CaTiO_3$ doped with 12.0 wt% Bi_2O_3–Li_2CO_3–H_3BO_3 sintered at 950 °C exhibits good microwave dielectric properties ($\varepsilon_r = 7.7$, $Q \times f = 11{,}300$ GHz, and $\tau_f = -5.0$ ppm/°C) [12]. In our previous study, by using nanopowders from high energy ball milling, Mg_2SiO_4-4 wt% LiF-24 wt% TiO_2 ceramics were achieved at 950 °C and possessed dielectric properties of $\varepsilon_r = 7.5$, $Q \times f = 38{,}430$ GHz, and $\tau_f = -0.4$ ppm/°C [13].

Li_2CO_3, Bi_2O_3 and LiF have been usually used as good candidate sintering additive owning to their low melting point [14–16]. Furthermore, $Ca_{0.8}Sm_{0.4/3}TiO_3$ (CST, $\varepsilon_r \sim 120$, $Q \times f \sim 13{,}800$ GHz, and $\tau_f \sim 400$ ppm/°C) which was reported as a τ_f compensator was selected as a further addition to adjust temperature coefficient of resonant frequency (τ_f) [17]. In this work, the substitution of Li and Bi for Mg was explored because the ionic radius of Li^+ (0.76 Å) and Bi^{3+} (1.03 Å) are similar to that of Mg^{2+} (0.72 Å). The fabrication of $[Mg_{1-x}(Li_{0.5}Bi_{0.5})_x]_2SiO_4$

($0 \le x \le 0.06$) was to improve sinterability of Mg_2SiO_4 ceramic. In addition, the τ_f compensator $Ca_{0.8}Sm_{0.4/3}TiO_3$ and sintering aid LiF were also added to $[Mg_{1-x}(Li_{0.5}Bi_{0.5})_x]_2SiO_4$. The effects of $Ca_{0.8}Sm_{0.4/3}TiO_3$ and LiF on the sintering characteristics, microstructures, crystal compositions and microwave dielectric properties of $(1-y)[Mg_{0.98}(Li_{0.5}Bi_{0.5})_{0.02}]_2SiO_4$-$yCa_{0.8}Sm_{0.4/3}TiO_3$-4 wt% LiF composite ceramics were investigated systematically.

2 Experimental procedure

Both $[Mg_{1-x}(Li_{0.5}Bi_{0.5})_x]_2SiO_4$ (MLBS, $0 \le x \le 0.06$) and $Ca_{0.8}Sm_{0.4/3}TiO_3$ (CST) composite ceramics were individually synthesized via a conventional solid-state reaction method using high-purity powders (> 99.9%) of MgO, SiO_2, Li_2CO_3, Bi_2O_3, $CaCO_3$, Sm_2O_3, TiO_2 and LiF. Predried raw materials were individually weighed according to the stoichiometric:$[Mg_{1-x}(Li_{0.5}Bi_{0.5})_x]_2SiO_4$ ($0 \le x \le 0.06$) and $Ca_{0.8}Sm_{0.4/3}TiO_3$ and then mixed in alcohol medium using zirconia ball for 8 h. All the mixtures were dried and calcined at 1200 °C for 4 h. Then, $(1-y)[Mg_{0.98}(Li_{0.5}Bi_{0.5})_{0.02}]_2SiO_4$-$yCa_{0.8}Sm_{0.4/3}TiO_3$-4 wt% LiF [(1-$y$)MLBS2-$y$CST, $0.05 \le y \le 0.2$] were prepared by mixing the MLBS2, CST and LiF powders at several weight ratios. The mixtures were reground by ball milling for 8 h, dried, mixed with 5 wt% PVA binder, and pressed under the pressure of 200 MPa into disks measuring 11.5 mm in diameter and about 6 mm in height. The pellets were sintered at 850–950 °C for 4 h in air at a heating rate of 3 °C/min.

The phase structure of the sintered ceramics were analyzed by the X-ray diffraction (XRD, Model Rigaku D/max 2550X, Japan) with CuK_α radiation. The microstructures of the samples were investigated using a scanning electron microscope (SEM; FEI Quanta 200, FEI company, Eindoven, Holland) coupled with energy dispersive X-ray spectroscopy (EDS). The bulk densities of the sintered ceramics were measured by the Archimedes method. The microwave dielectric properties of the sintered pellets were measured using a network analyzer (ZVB20, Rohde & Schwarz, Munich, Germany) with the $TE_{01\delta}$ cavity method. The temperature coefficient of resonant frequency (τ_f) was calculated with the following equation:

$$\tau_f = \frac{(f_{80} - f_{20})}{f_{20}(T_{80} - T_{20})} \times 10^6 \ (\text{ppm/°C})$$

where f_{80} and f_{20} are the resonant frequency at T_{80} and T_{20}, respectively.

3 Results and discussion

3.1 $[Mg_{1-x}(Li_{0.5}Bi_{0.5})_x]_2SiO_4$ system

Figure 1 gives the XRD patterns of $[Mg_{1-x}(Li_{0.5}Bi_{0.5})_x]_2SiO_4$ ($0 \le x \le 0.06$) ceramics sintered at 1350 °C. As shown in Fig. 1a, all the main peaks can be indexed using the forsterite Mg_2SiO_4 (JCPDS#78-1371), along with small amounts of MgO as the secondary phase. After added Li^+ and Bi^{3+}, the pure Mg_2SiO_4 phase could be obtained which suggests that addition of Li^+ and Bi^{3+} effectively inhibits the generation of the second phase. As shown in the right of Fig. 1, the position of (112) peak of $[Mg_{1-x}(Li_{0.5}Bi_{0.5})_x]_2SiO_4$ ($0 \le x \le 0.06$) shifted slightly toward the lower angles with $x \le 0.04$, suggesting an increase in the crystalline interplanar spacing of (112) due to the substitution of Li^+ (0.76 Å, CN = 6) or Bi^{3+} (1.03 Å, CN = 6) for Mg^{2+} (0.72 Å, CN = 6).

Figure 2 presents the SEM images of as-fired surface of $[Mg_{1-x}(Li_{0.5}Bi_{0.5})_x]_2SiO_4$ ceramics. It is obvious that with increasing x, the grain size increases. The average grain size of Fig. 2a–d, which is measured by the liner intercept method [18], is to be 3.18, 5.06, 10.48 and 16.63 μm, respectively. Thus, addition of Li and Bi to Mg_2SiO_4 ceramics facilitates grain growth and lowers the sintering temperature from 1540 to 1350 °C.

Figure 3 displays the bulk density and microwave dielectric properties of $[Mg_{1-x}(Li_{0.5}Bi_{0.5})_x]_2SiO_4$ ($0.02 \le x \le 0.06$) ceramics as functions of sintering temperatures and composition x. Microwave dielectric properties of $[Mg_{1-x}(Li_{0.5}Bi_{0.5})_x]_2SiO_4$ ceramics with various x sintered at their optimal temperatures are presented in Table 1. As shown in Fig. 3a, for $x = 0.02$, the bulk density of sintered ceramics increased, and then declined after reaching a maximum (1350 °C) with increasing sintering temperature. For $x = 0.04$ and

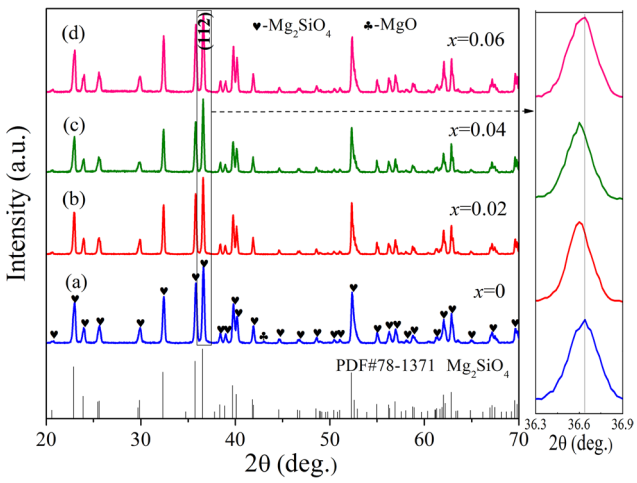

Fig. 1 The X-ray diffraction patterns of the $[Mg_{1-x}(Li_{0.5}Bi_{0.5})_x]_2SiO_4$ ($0 \le x \le 0.06$) ceramics sintered at 1350 °C for 4 h

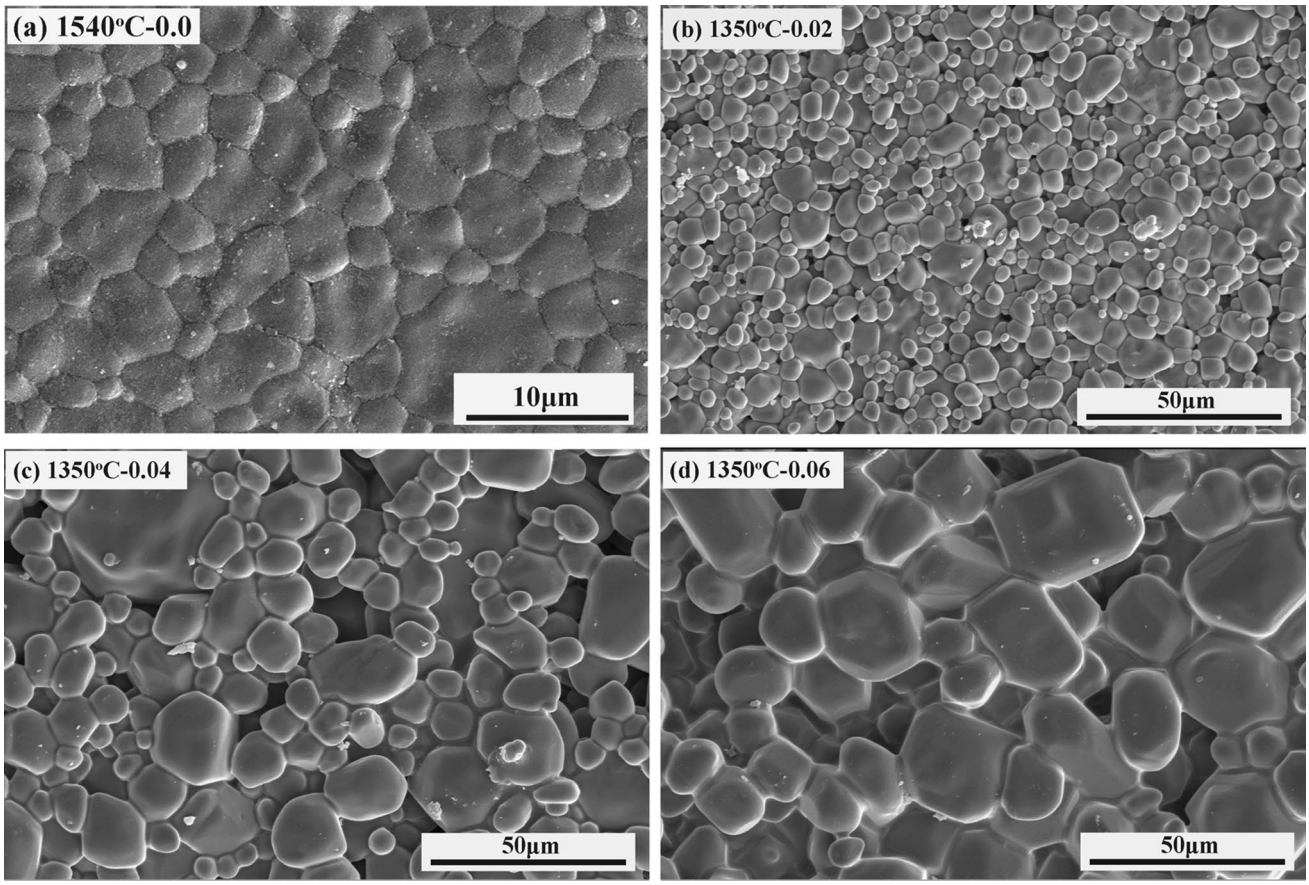

Fig. 2 SEM images of as-fired surface of $[Mg_{1-x}(Li_{0.5}Bi_{0.5})_x]_2SiO_4$ ceramics: **a** $x=0.0$, 1540 °C; **b** $x=0.02$, 1350 °C; **c** $x=0.04$, 1350 °C; **d** $x=0.06$, 1350 °C

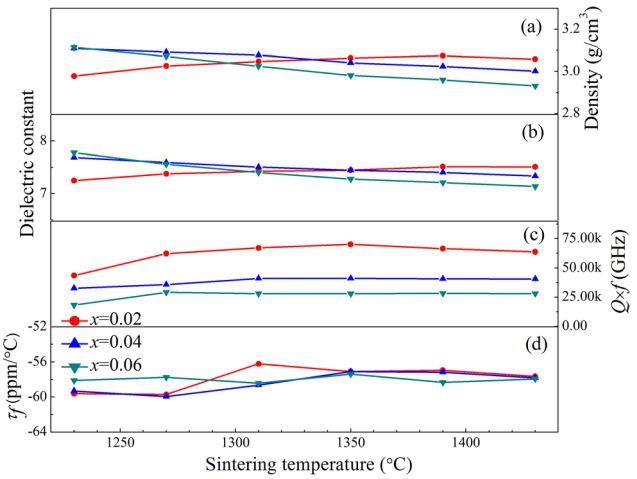

Fig. 3 (*a*) The bulk density, (*b*) ε_r values, (*c*) $Q\times f$ values and (*d*) τ_f values of $[Mg_{1-x}(Li_{0.5}Bi_{0.5})_x]_2SiO_4$ ($0.02\le x\le 0.06$) ceramics sintered at different temperatures

Table 1 Microwave dielectric properties of $[Mg_{1-x}(Li_{0.5}Bi_{0.5})_x]_2SiO_4$ ceramics sintered at optimal temperature with various x values

x value	Ts (°C)	The bulk density (g/cm^3)	ε_r	$Q\times f$ (GHz)	τ_f (ppm/°C)
0	1540	3.12	7.7	147,000	−59
0.02	1350	3.06	7.4	70,088	−57
0.04	1310	3.08	7.5	41,084	−59
0.06	1270	3.07	7.6	29,197	−58

0.06, declination of bulk density with sintering temperature is related to the evaporation of lithium and bismuth at elevated temperature [19]. As shown in Table 1 and Fig. 3a, the optimized densification temperatures lowered from 1350 to 1270 °C with increasing x from 0.02 to 0.06 which suggests that the substitution of Mg by Li and Bi effectively lowers the sintering temperature and broadens the sintering range of Mg_2SiO_4 ceramics. In Fig. 3b, the variations in ε_r values with sintering temperatures shown a similar trend with that of bulk density. With the increase of x from 0.02 to 0.06, ε_r values nearly unchanged with sintering temperature

from 1230 to 1430 °C. As is well-known, quality factor is related to intrinsic parameters such as densification, secondary phase, lattice defects, impurity, and microstructure characteristics [20]. For $x = 0.02$ in Fig. 3c, with the increase of sintering temperature, the $Q \times f$ values of the samples first increased and then decreased slightly. Basically, the $Q \times f$ values decreased with x and remained nearly constant within the sintering temperature range. Figure 3d shows that the τ_f values of $[Mg_{1-x}(Li_{0.5}Bi_{0.5})_x]_2SiO_4$ ceramics did not change remarkably with sintering temperature and x. It maintained stable at about −57 to −59 ppm/°C. $[Mg_{0.98}(Li_{0.5}Bi_{0.5})_{0.02}]_2SiO_4$ (MLBS2) ceramics at 1350 °C shown good microwave dielectric properties of $\varepsilon_r = 7.4$, $Q \times f = 70{,}088$ GHz, and $\tau_f = -57$ ppm/°C.

3.2 (1-y)$[Mg_{0.98}(Li_{0.5}Bi_{0.5})_{0.02}]_2SiO_4$–y$Ca_{0.8}Sm_{0.4/3}TiO_3$ system

In order to adjust the temperature coefficient of resonant frequency (τ_f) to near-zero and lower the sintering temperature below 950 °C, LiF added $(1-y)$MLBS2-yCST $(0.05 \le y \le 0.2)$ composite ceramics were explored. Figure 4 gives the XRD patterns of $(1-y)$MLBS2-yCST-4.0 wt% LiF ceramics sintered at 875 °C for 4 h. The XRD patterns present a multiphase system with a forsterite MLBS2 (JCPDS#78-1371) and a perovskite CST (JCPDS#78-1013), including small amounts of MgO, SiO_2, and $MgSiO_3$ phases which would influence the dielectric properties of ceramics. With increasing composition y, the intensities of the diffraction peaks of CST phase reinforce, and the intensities of the diffraction peaks of MLBS2 phase weaken.

Figure 5 exhibits the SEM micrographs of fractured surface of $(1-y)$MLBS2-yCST-4.0 wt% LiF $(0.05 \le y \le 0.2)$ ceramics sintered at 875 °C as a function of y. As shown in Fig. 5a–d, all simples have a well-densified microstructure with only a few pores. Furthermore, there are two kinds different size grains as marked in Fig. 5c. The EDS analysis (Fig. 5e, f) illustrates the larger grain A is turned out to be MLBS2 and the smaller grain B is CST phase, which is in accordance with the XRD phase composition analysis.

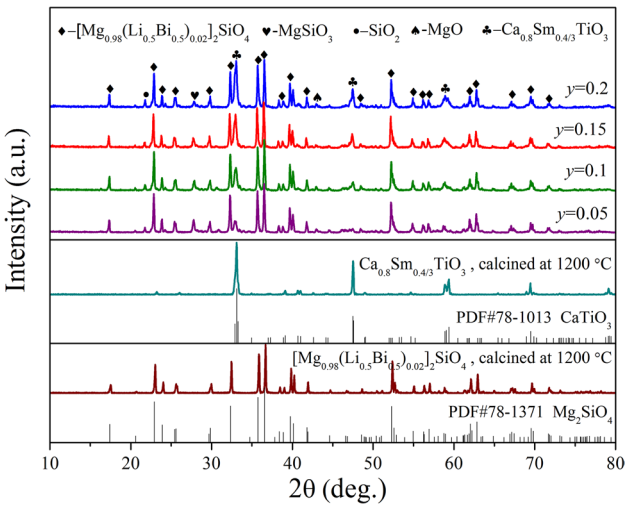

Fig. 4 The X-ray diffraction patterns of the $(1-y)$MLBS2-yCST-4 wt% LiF $(0.05 \le x \le 0.2)$ ceramics sintered at 875 °C for 4 h

Figure 6 presents the bulk densities, dielectric constant and $Q \times f$ values of the $(1-y)$MLBS2-yCST-4.0 wt% LiF $(0.05 \le y \le 0.2)$ ceramics as functions of sintering temperatures and y. It is seen in Fig. 6a that as sintering temperature increased from 850 to 950 °C, the bulk density of sintered ceramics with $y = 0.15$ increased first and then reached a maximum value of 3.17 g/cm^3 at 875 °C. Thus, for y = 0.15 and 0.2, LiF effectively lowered the sintering temperature of MLBS2-CST ceramics to a wide temperature range (850–950 °C). The good effect of LiF on the sinterability of the ceramics may be related to the substitution of F^- (1.33 Å) for O^{2-} (1.4 Å) [21]. As displayed in Fig. 6b, c, the variations in ε_r and $Q \times f$ values with sintering temperatures are consistent with that of bulk density, which suggests that the bulk density is the leading factor to control ε_r and $Q \times f$ values in MLBS2-CST ceramics. With the increasing of y from 0.05 to 0.2, ε_r increases from 10.6 to 12.6, connected with higher ε_r values of CST (ε_r ~ 120). With increasing sintering temperature, the $Q \times f$ values increased to a maximum value of 12,000 GHz for 0.85MLBS2-0.15CST-4 wt% LiF ceramics sintered at 875 °C for 4 h. As shown in Fig. 6c, at a fixed sintering temperature, $Q \times f$ values increased with y to 0.15, and then slightly decreased for $x = 0.2$.

Figure 7 shows the τ_f values of $(1-y)$MLBS2-yCST-4 wt% LiF ceramics sintered at different temperatures. The temperature coefficient of resonant frequency (τ_f) is related to the composition, the additives, and the second phase of the materials [22]. At fixed y, the τ_f values of the composite ceramics were not significant changed with sintering temperature and τ_f was adjusted from negative to positive when the y value increases from 0.05 to 0.2 owing to the large positive τ_f value of CST (τ_f ~400 ppm/°C). A near-zero τ_f value of +4.9 ppm/°C was obtained for 0.85MLBS2-0.15CST-4 wt% LiF ceramics sintered at 875 °C.

Figure 8 provides XRD pattern, SEM image and EDS analyses of 0.85MLBS2-0.15CST-4 wt% LiF composite ceramics co-fired with 20 wt% silver (Ag) powders sintered at 875 °C for 4 h. It can be seen that multiphase of MLBS2, CST and respective metals (Ag) were observed. And other peak in the XRD pattern could not be detected, indicating that there is no chemical reaction between Ag powders and 0.85 MLBS2–0.15 CST-4 wt% LiF ceramics. Therefore, 0.85 MLBS2–0.15 CST-4 wt% LiF composite ceramic is a suitable candidate for LTCC application.

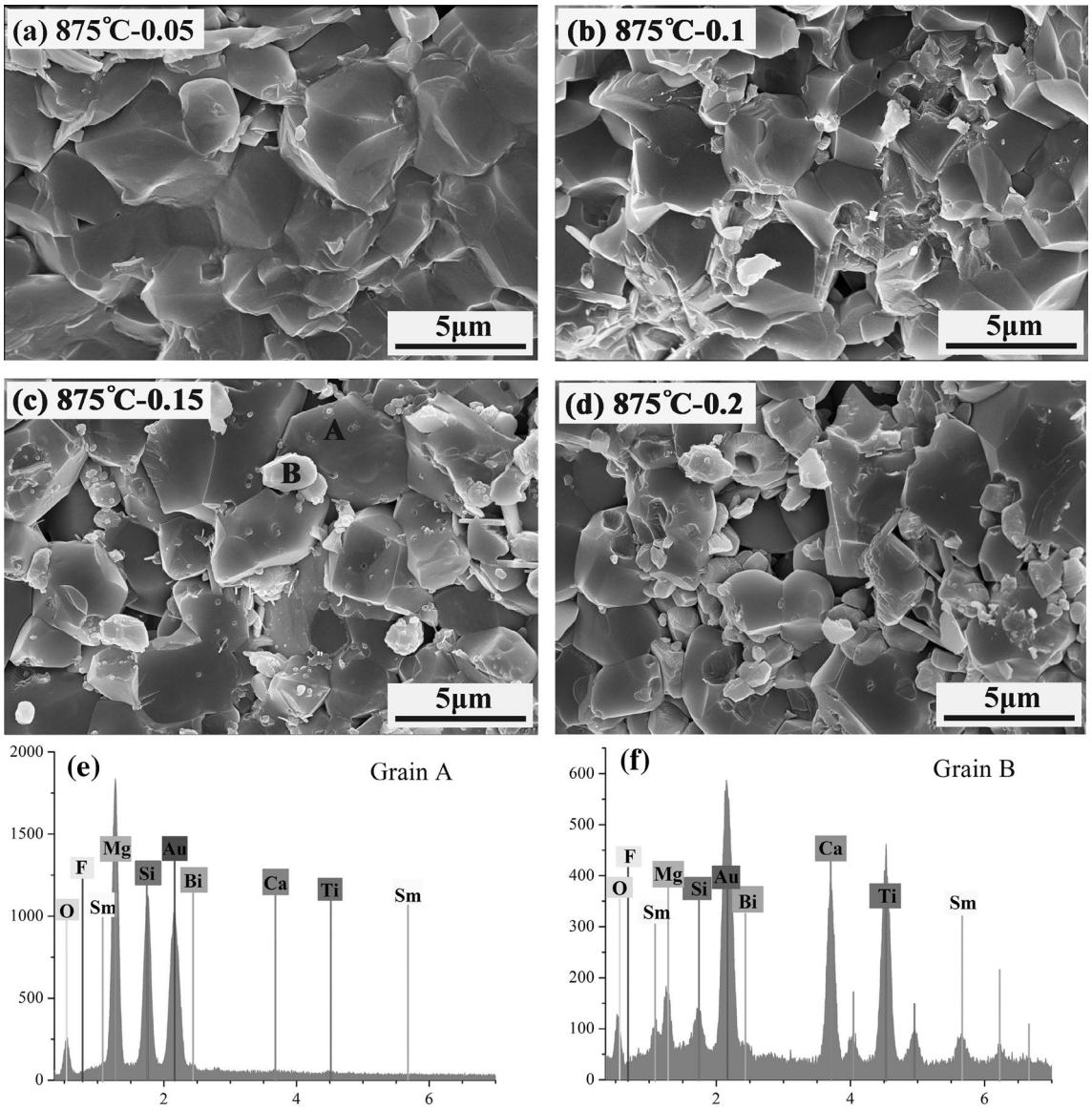

Fig. 5 SEM images of fractured surface of (1-*y*)MLBS2-*y*CST-4 wt% LiF ceramics sintered at 875 °C: **a** $y=0.05$, **b** $y=0.1$, **c** $y=0.15$, **d** $y=0.2$. EDS spectrums of **e** grain A marked in **c** and **f** grain B marked in **c**

4 Conclusions

$[Mg_{1-x}(Li_{0.5}Bi_{0.5})_x]_2SiO_4$ ($0 \le x \le 0.06$) ceramics were prepared by a conventional solid-state reaction route and the sintering characteristics, microstructures, crystal compositions and microwave dielectric properties were investigated. The introduction of Li^+ and Bi^{3+} successfully optimized the sinterability of the ceramic and lowered the sintering temperature from 1540 to 1350 °C. The $[Mg_{0.98}(Li_{0.5}Bi_{0.5})_{0.02}]_2SiO_4$ ceramics sintered at 1350 °C showed good microwave dielectric properties: $\varepsilon_r=7.4$, $Q\times f=70{,}088$ GHz, and $\tau_f=-57$ ppm/°C. In addition, the $(1-y)[Mg_{0.98}(Li_{0.5}Bi_{0.5})_{0.02}]_2SiO_4$-$yCa_{0.8}Sm_{0.4/3}TiO_3$ ($0.05 \le y \le 0.2$) composite ceramics added with 4 wt% LiF were well sintered from 850 to 950 °C. High performance of microwave dielectric properties could be obtained in the $0.85[Mg_{0.98}(Li_{0.5}Bi_{0.5})_{0.02}]_2SiO_4$-$0.15Ca_{0.8}Sm_{0.4/3}TiO_3$-4 wt% LiF composite ceramic sintered at 875 °C for 4 h with a permittivity value of 11.9, a $Q\times f$ value of 12,000 GHz (at 8.6 GHz), and a τ_f value of 4.9 ppm/°C. The XRD result, SEM image and EDS analyses proved that $0.85[Mg_{0.98}(Li_{0.5}Bi_{0.5})_{0.02}]_2SiO_4$-$0.15Ca_{0.8}Sm_{0.4/3}TiO_3$-4 wt% LiF composite ceramics were co-fired well with silver (Ag) powders at 875 °C, indicating the composite ceramic is a suitable candidate for LTCC application.

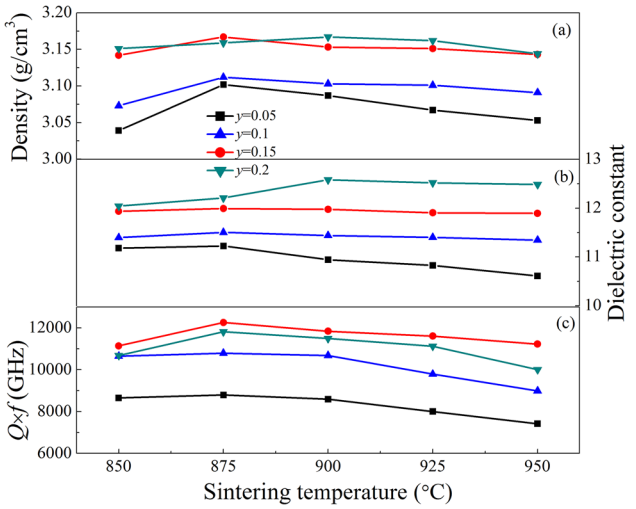

Fig. 6 (*a*) The bulk density, (*b*) ε_r values and (*c*) $Q\times f$ values of $(1-y)$MLBS2-*y*CST-4 wt% LiF ceramics sintered at different temperatures

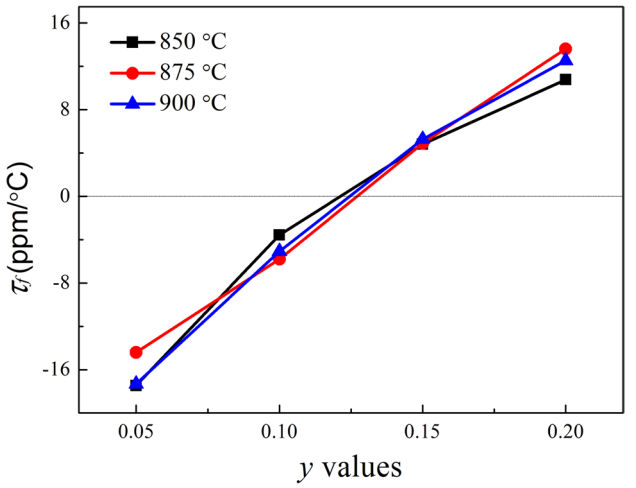

Fig. 7 τ_f values of $(1-y)$MLBS2-*y*CST-4 wt% LiF ceramics sintered at different temperatures

Acknowledgements This work is supported by the National Natural Science Foundation of China (Grant Nos.: 51572165, 51602005).

References

1. D. Thomas, P. Abhilash, M.T. Sebastian, J. Eur. Ceram. Soc. **33**, 87 (2013)

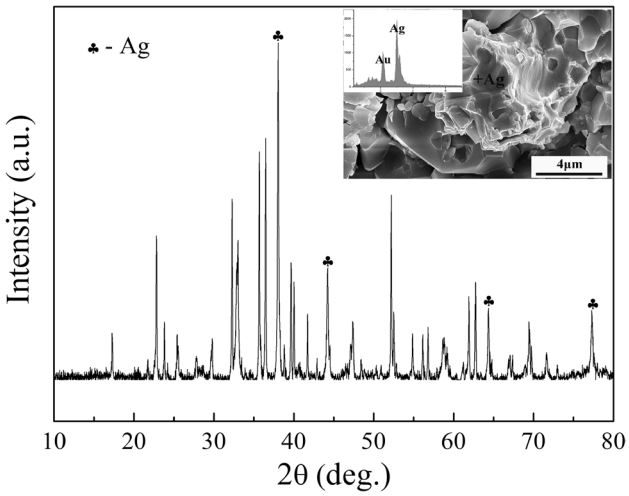

Fig. 8 The XRD pattern, SEM image and EDS spectrum of 0.85MLBS2-0.15CST-4 wt% LiF ceramic mixed with 20 wt% Ag powders sintered at 875 °C for 4 h

2. M.T. Sebastian, H. Jantunen, Int. Mater. Rev. **53**, 57 (2008)
3. M. Guo, G. Dou, S.P. Gong, D.X. Zhou, J. Eurp. Ceram. Soc. **32**, 883 (2012)
4. L.X. Pang, D. Zhou, J. Guo, Z.M. Qi, T. Shao, Ceram. Int. **39**, 4719 (2013)
5. T. Tsunooka, M. Androu, Y. Higashida, H. Sugiura, H. Ohsato, J. Eurp. Ceram. Soc. **23**, 2573 (2003)
6. C. Zhang, R.Z. Zuo, J. Zhang, Y. Wang, J. Am. Ceram. Soc. **98**, 707 (2015)
7. Z.F. Fu, P. Liu, J.L. Ma, X.G. Zhao, H,W Zhang, Mater. Chem. Phys. **170**, 118 (2016)
8. J. Sugihara, K. Kakimoto, I. Kagomiya, H. Ohsato, J. Eurp. Ceram. Soc. **27**, 3105 (2007)
9. L. Liu, Y.B. Feng, T. Qiu, X.Y. Li, J. Mater. Sci. Mater. Electron **26**, 1316 (2015)
10. S.Q. Meng, Z.X. Yue, H. Zhuang, F. Zhao, L.T. Li, J. Am. Ceram. Soc. **93**, 359 (2010)
11. J. Li, P. Liu, Z.F. Fu, Q.Q. Feng, J. Alloys Compd. **660**, 93 (2016)
12. G. Dou, D.X. Zhou, M. Guo, S.P. Gong, Y.X. Hu, J. Mater. Sci. Mater. Electron **24**, 1431 (2013)
13. J.L. Ma, T. Yang, Z.F. Fu, L. Peng, Q.Q. Feng, L.P. Zhao, J. Alloys Compd. **695**, 3198 (2017)
14. G.F. Fan, M.B. Shi, W.Z. Lu, Y.Q. Wang, F. Liang, J. Eurp. Ceram. Soc. **34**, 23 (2014)
15. V. Gil, J. Tartaj, C. Moure, P. Duran, Ceram. Int. **33**, 471 (2007)
16. X.J. Bai, P. Liu, Z.F. Fu, B.C. Guo, J. Alloys Compd. **667**, 146 (2016)
17. K.H. Yoon, W.S. Kim, E.S. Kim, Mater. Sci. Eng. **B99**, 112 (2003)
18. A. Thorvaldsen, Acta Mater. **45**, 595 (1997)
19. Y. Iida, J. Am. Ceram. Soc. **43**, 171 (1960)
20. H. Tamura, J. Eurp. Ceram. Soc. **26**, 1775 (2006)
21. Z.F. Fu, P. Liu, J.L. Ma, X.M. Chen, H.W. Zhang, Mater. Let. **146**, 436 (2016)
22. Y.B. Chen, J. Alloys Compd. **509**, 9226 (2011)